Pergamon

PII: S0277-5387(97)00085-5

Polyhedron Vol. 16, No. 18, pp. 3219–3233, 1997

0277–5387/97 $17.00+0.00

Understanding the binding and activation of thiophenic molecules in transition metal complexes and clusters

Suzanne Harris

Department of Chemistry, University of Wyoming, Laramie, WY 82071-3838, U.S.A.

Abstract—Organometallic complexes and clusters provide examples of binding modes of thiophenic molecules, activation of the C—S bond in thiophene, and actual desulfurization of thiophenic molecules. Our molecular orbital calculations on these complexes are aimed toward understanding how the binding and reactivity of the thiophenic ligands are influenced by the electronic structures of the various complexes. Results of Fenske–Hall molecular orbital calculations for complexes incorporating both η^5 and η^1 thiophene ligands show that although the thiophene ligand acts primarily as a donor, thiophene can and does act as a π acceptor under certain conditions. These results suggest how binding of a thiophenic ligand and/or activation of the C—S bond might be optimized in η^5 or η^1 complexes. Results for metal-inserted or ring opened complexes show distinct differences in the electronic structure of saturated and unsaturated complexes. The orbital structures and charge distributions provide explanations for the different reactivities of a number of these complexes. Comparisons of the electronic structures and reactivities of the metal-inserted complexes and the butterfly cluster $(Cp')_2Mo_2Co_2S_3(CO)_4$, which is known to remove sulfur from thiophene, suggest similarities in the mechanism of binding and activation of a thiophene ring in the complexes and the butterfly cluster. © 1997 Elsevier Science Ltd

Keywords: hydrodesulfurization; thiophene; electronic structure.

Understanding the mechanism of hydrodesulfurization (HDS) catalysis has been a goal of researchers for many years. While a complete understanding of the process has certainly not been achieved, the combined efforts of many research groups have added to our knowledge of the nature of the active catalysts and the possible ways that binding and activation of thiophenic molecules may occur on the active catalyst surfaces. Our research efforts are aimed at understanding both the electronic basis for the catalytic activity of certain binary and promoted transition metal sulfides and the role of electronic structure in binding and activation of thiophenic molecules at transition metal centers. Thus our current efforts include studies of the electronic structures of both relevant transition metal sulfide surfaces and molecular complexes that incorporate thiophenic ligands. This paper will focus on what we believe are some of the most important results from our molecular calculations.

While it has been clear for many years that understanding the HDS mechanism will require clarifying the mode of binding and activation of thiophene on an HDS catalyst, the complexity of the real catalytic systems (supported transition metal sulfide based materials at high temperatures and high H_2 pressures) has made it very difficult to achieve this step. Over the last 10 years, however, the organometallic chemistry community has shown a remarkable interest in the HDS problem, and the work of several research groups has led to a wealth of new model molecular complexes and clusters [1–3]. These model systems provide examples of numerous binding modes of thiophenic molecules, activation of the C—S bond in thiophene, and in some cases actual desulfurization of thiophenic molecules. Our own efforts in the area of model molecular systems began with a general study of the electronic structure of complexes exhibiting different metal-thiophene binding modes [4]. Recently, we have considered a number of these systems in greater depth and have begun to develop a better understanding of the role of electronic factors in activation of thiophenic rings [5,6]. We have also begun to study metal–sulfur clusters which also provide model systems for HDS catalysis.

This paper will review some of our results and discuss factors which appear to be related to the reactivity of metal–thiophene complexes. After a brief description of the calculational method, the next sections of the paper summarize some of what we consider to be important results of our calculations. These results provide insights into the role of the metal center, ancillary ligands, coordination geometries (around the metal), and coordination mode of the thiophenic ligand in C—S bond activation. The electronic structures of complexes incorporating η^5, η^1, and ring-opened thiophene ligands are discussed. The η^5 and η^1 binding modes were of initial interest because researchers had debated for many years whether thiophene might bind to an HDS catalyst surface through one of these modes. The η^5 mode proved to be of particular interest when it was demonstrated that bound thiophene often shows reactivity not observed in free thiophene [7,8]. A number of transition metal complexes incorporating η^1 or S-bound thiophene have also been characterized [9–12]. Although the S-bound thiophenic ligands do not exhibit ring activation in these stable complexes, Jones and coworkers showed that an S-bound intermediate serves as the precursor to a number of Rh-inserted thiophenic complexes [13]. Ring opened complexes have also been synthesized by Merola [14], Bianchini [15,16], Maitlis [17], Angelici [18], and Field [19]. Several of these complexes show truly novel and remarkable reactivity. Bianchini [20] and Maitlis [21] have achieved complete desulfurization of thiophenic rings, starting with ring opened Ir and Pt complexes, respectively.

Recently we have also begun to consider the electronic structure of several clusters which have proved useful in modeling HDS reactions. The 'butterfly' cluster $(Cp')_2Mo_2Co_2S_3(CO)_4$, ($Cp' = CH_3C_5H_4$) is of particular interest, since the Curtis group has shown that this cluster removes sulfur from thiophene to form the cubane cluster $(Cp')_2Mo_2Co_2S_4(CO)_2$ [22,23]. The composition of the butterfly cluster makes it a particularly attractive model for the promoted Co/Mo/S HDS catalysts. We have carried out a series of calculations related to this and other model clusters, and some of our results are summarized here.

Calculational details

All of the results described here were obtained from Fenske-Hall [24] molecular orbital calculations. Mulliken populations analyses were used to determine orbital populations and atomic charges [25].

The 1s through *n*d functions for all of the transition metals were generated by a best fit to Herman–Skillman atomic calculations [26] using the method of Bursten, Jensen, and Fenske [27]. The $(n+1)$s and $(n+1)$p functions were chosen to have exponents of 2.0, 2.2, and 2.4 for the 3d, 4d, and 5d metals, respectively. The carbon and sulfur functions were taken from the double-ζ functions of Clementi [28]. The valence p functions were retained as the double-ζ functions, while all the other functions were reduced to single-ζ functions. An exponent of 1.2 was used for hydrogen.

The molecular structures of all the complexes and clusters described here have been determined by X-ray diffraction. These known structures were used for the molecular orbital calculations.

DISCUSSION

η^5-Bound thiophene

The earliest characterized complexes incorporating thiophene ligands were those containing η^5-bound thiophene, and we began our investigations with these complexes. Since the π system of the thiophene ring exhibits an orbital structure analogous to that of Cp^- (Fig. 1) it is not surprising that nearly all of the characterized η^5-thiophene complexes have η^5–Cp analogs. Comparisons among the electronic structures of $Cr(CO)_3T$ (T = thiophene), $[Mn(CO)_3T]^+$, $[RuCpT]^+$, $[RuT_2]^{2+}$, and $[RuTMT_2]^{2+}$ (TMT = tetramethyl thiophene) and analogous η^5–Cp complexes revealed several differences in the donor and acceptor properties of thiophene and Cp^- [4]. In Cp^-, the primary donor orbitals are the degenerate HOMO e_1'' orbitals, while the LUMO e_2'' orbitals can serve as acceptors. In thiophene the corresponding $1a_2$ and $2b_1$ orbitals serve as donors while the unoccupied $3b_1$ and $2a_2$ orbitals serve as acceptors. Comparisons of the bonding in similar $M(CO)_3L$, $L = Cp^-$ or T, complexes showed that Cp^- is a better donor and poorer acceptor than thiophene. This results primarily from the relative energies of the ligand orbitals. The energies of the acceptor orbitals are particularly important, since the thiophene $3b_1$ acceptor orbital is approximately 7 eV lower in energy than the $Cp^- e_2''$ orbitals. Thiophene is generally considered to bind more weakly than Cp^- to transition metal centers, and our results suggest that in complexes where binding depends primarily on donation to the metal center the weaker binding is a consequence of the poorer donor ability of thiophene. We observed, however, that for the larger 4*d* and 5*d* metals, the stronger interactions between the large sulfur orbitals and the metal d orbitals lead to stronger metal–thiophene binding. In addition, we found that when thiophene and a better donor are simultaneously bound to a transition metal center, the acceptor ability of thiophene leads to stronger metal–thiophene binding. Overall, this means that η^5-thiophene binding should be strongest in complexes incorporating thiophene, a 4d or 5d metal, and donor ligands. This conclusion is consistent with a number of findings by the Rauchfuss group [29,30].

It has been shown that η^5-bound thiophene is in some cases activated toward nucleophilic attack [7,8], and one might assume that changes in the electronic structure of the coordinated thiophene ring are responsible for the activation. Our calculations

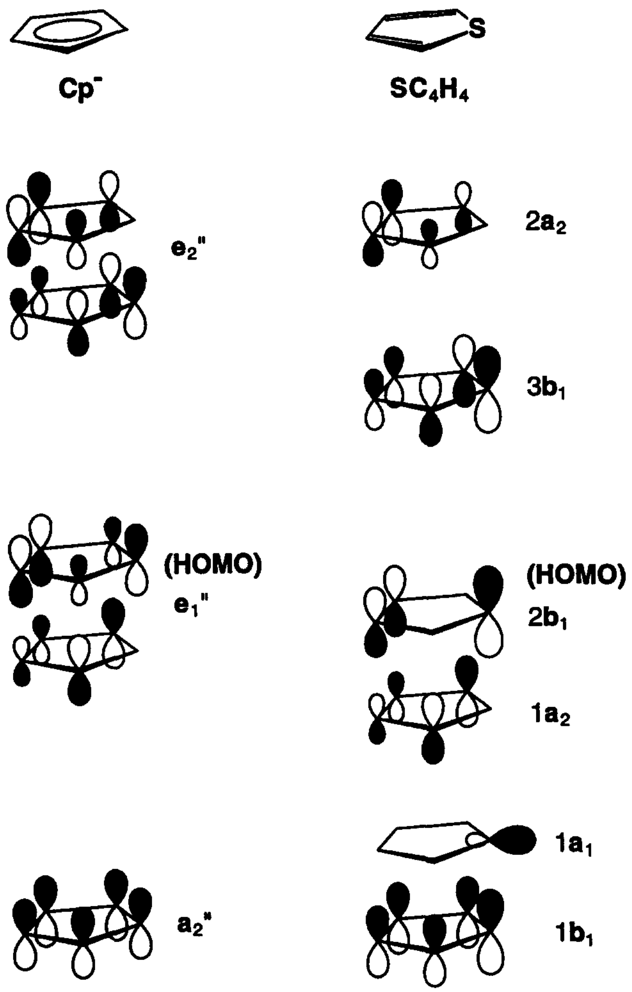

Fig. 1. Comparison of the high energy occupied and low energy unoccupied orbitals of cyclopentadienyl anion and thiophene. (Ref. [4]).

revealed only small perturbations of the thiophene electronic structure upon η^5 coordination. This, coupled with the fact that the ring is only activated in positively charged complexes, led us to suggest that the charge alone is probably responsible for activation of the ring. If this is true, it raises the question whether the chemistry of these η^5 complexes is really similar to the chemistry occurring on the HDS catalysts.

η^1-Bound thiophene

Several S-bound thiophene and dibenzothiophene (DBT) complexes have been characterized. These complexes incorporate several different transition metals (although all of the metals are formally d^6) and both donor and acceptor ligands. In all of these complexes the thiophenic ligands display pyramidal bonding around the thiophenic sulfur. As a result, the transition metal and the thiophene ring do not lie in the same plane (see Fig. 2). It is somewhat surprising, however, that even though all the complexes shown in Fig. 2 exhibit a tilted thiophenic ligand, the tilt angle actually varies by over 20°. Calculations showed that the tilted or tipped configuration is related to the type and strength of metal sulfur interactions found in these complexes [5].

In the η^1(S) binding mode, thiophene (or DBT) can serve as both a σ and π donor, since ligand to metal donation might occur from either the $2b_1(\pi)$ or $1a_1(\sigma)$ orbital. At the same time, thiophene or DBT also has the potential to act as a π acceptor through the $3b_1$ π^* LUMO. Calculations on the S-bound complexes in Fig. 2 showed, however, that the M–S bonding is dominated by thiophene's donor capabilities, and that the tilt of the ligand can be attributed to thiophene acting as a two rather than four electron donor. That is, donation from the filled $2b_1$ π orbital is unnecessary and undesirable when the thiophenic ligands bind to these 16-electron CpL_2M fragments. Using the molec-

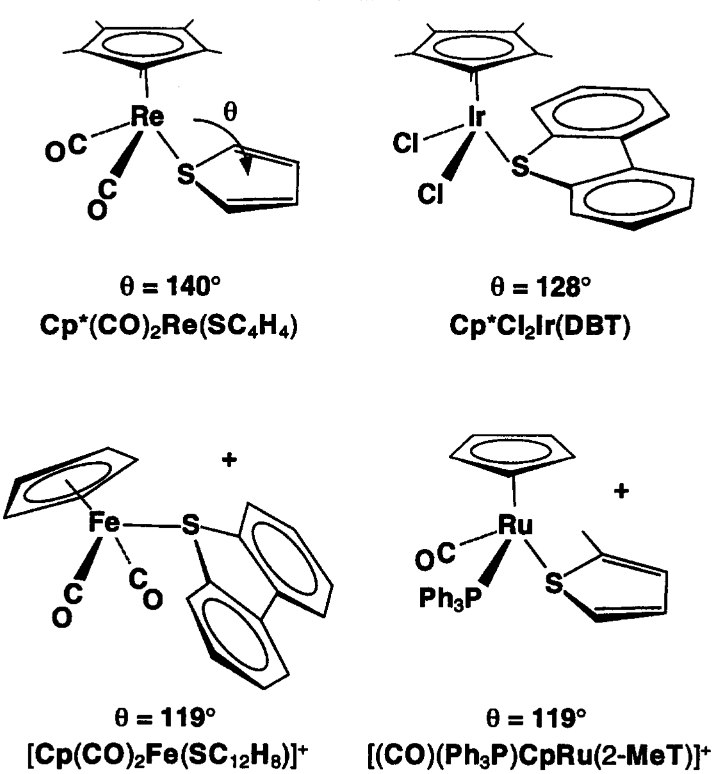

θ = 140°
$Cp^*(CO)_2Re(SC_4H_4)$

θ = 128°
$Cp^*Cl_2Ir(DBT)$

θ = 119°
$[Cp(CO)_2Fe(SC_{12}H_8)]^+$

θ = 119°
$[(CO)(Ph_3P)CpRu(2\text{-}MeT)]^+$

Fig. 2. Structures of η^1(S-)bound thiophene and dibenzothiophene complexes. The angle θ measures the angle between the metal–sulfur bond and a line connecting the sulfur atom and the midpoint of the opposite side of the five-membered thiophene ring.

ular orbital diagram of $Cp(CO)_2ReT$ (Fig. 3) as an example, we can see that while a planar configuration about the ring sulfur would enable the sulfur $1a_1$ σ lone pair to donate most effectively into the unoccupied metal d_{z^2} type orbital, this planar configuration would also lead to a strong antibonding interaction between the sulfur $2b_1$ π lone pair and the occupied metal d_{yz} orbital. Bending at the sulfur decreases both the a_1–d_{z^2} σ bonding and $2b_1$–d_{yz} π antibonding interaction, but it also allows the filled $2b_1$ π orbital to overlap with and donate into the empty metal d_{z^2} orbital. Thus, bending at the sulfur alleviates an antibonding interaction with the metal d_{yz} orbital and allows both the σ and π ligand donor orbitals to interact with the empty metal d_{z^2} orbital. The net result is the 'donation' of two rather than four electrons to the metal.

It is important to recognize that a more planar configuration of the ring would allow back-donation from the metal d_{yz} orbital into the unoccupied thiophene $3b_1$ π^* LUMO, thus canceling out at least some of the π donor antibonding interaction. The relative importance of the π donor and π acceptor interactions depend, however, on the energy separations between the filled metal d_{yz} orbital and the occupied and unoccupied ligand π orbitals (these are labeled E(M-π) and E(M-π^*), respectively, in Fig. 3). The three fragment π orbitals, metal d_{yz}, thiophene $2b_1$ and thiophene $3b_1$, combine in the complex to form the m.o.'s labeled $1a'$, $2a'$, and $3a'$. The lowest, $1a'$, is primarily thiophene $2b_1$ in character and is bonding between the metal and thiophene; the highest, $3a'$, is primarily thiophene $3b_1$ in character and is antibonding between the metal and thiophene. The $3a'$ orbital forms the LUMO of the complex. The middle orbital, $2a'$, which is occupied, is *antibonding* between the metal d_{yz} and thiophene $2b_1$ orbitals and *bonding* between the metal d_{yz} and thiophene $3b_1$ orbitals. The fragment orbital character of this molecular orbital depends on the relative magnitudes of E(M-π) and E(M-π^*). Our calculations for this group of complexes show that the 'tilt' angle of the thiophene ring actually provides a good measure of both the relative magnitudes of E(M-π) and E(M-π^*) and the relative participation of the thiophene π and π^* orbitals in the $2a'$ molecular orbital. At an extreme where E(M-π) is much smaller than E(M-π^*), there will be little interaction between the metal and the π^* thiophene orbitals. The only mechanism for decreasing the resulting metal–thiophene antibonding interaction will involve tilting the ring, which decreases the overlap and antibonding interaction between the metal d_{yz} and thiophene $2b_1$ orbitals. At the other extreme, where E(M-π) is much larger than E(M-π^*), the bonding interaction between the metal d_{yz} and thiophene π^* orbitals will increase and become more important than the antibonding interaction between the filled metal and thiophene π orbitals. This bonding interaction (or π back donation) is optimized

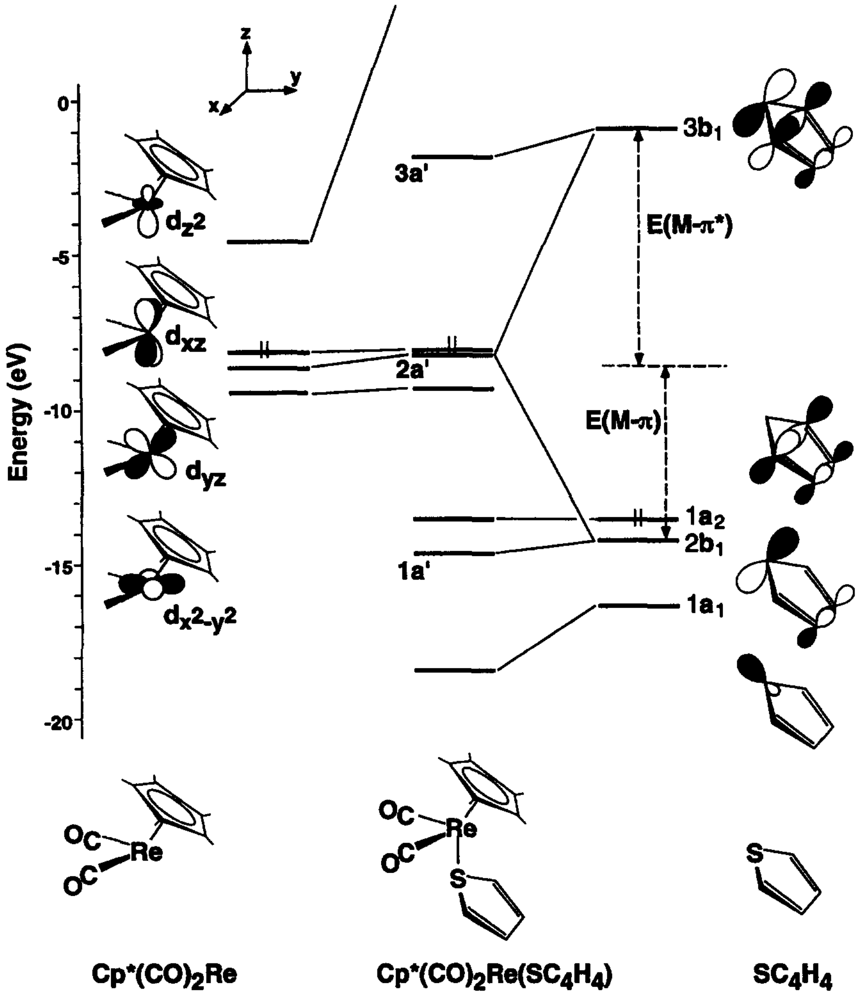

Fig. 3. Calculated energy level diagram for $Cp^*(CO)_2Re(SC_4H_4)$ and for the $Cp^*(CO)_2Re$ and SC_4H_4 fragments. See text for discussion of E(M-π) and E(M-π*).

by a flat tilt angle. The relative tilt angle therefore should provide a measure of both the two energy separations and the importance of π back donation in each complex. The calculated orbital structures of the complexes in Fig. 2 show such a correlation among the tilt angle, the relative magnitudes of E(M-π) and E(M-π*) energies, and the fragment orbital character of the 2*a*′ molecular orbital.

In the Re complex, where E(M-π*) is smallest, (the energy of the occupied d_{yz} orbital lies approximately midway between the energies of the ligand π donor and acceptor orbitals), both the π donor and π* acceptor ligand orbitals interact with the metal d_{yz} orbital. Weak π back donation tends to cancel out the antibonding interaction between the two occupied orbitals. This stabilizes the 2*a*′ orbitals so that it becomes the second highest occupied molecular orbital (SHOMO) in the Re complex. Thus in the Re complex participation of the π* orbital is maximized, and the tilt of the ring is smallest. In the Fe and Ru complexes, where E(M-π*) is considerably larger, the interaction between the filled d_{yz} and empty π* orbital becomes negligible, and the tilt of the ring increases by about 20°. In the Ir complex (note the donor ligands), E(M-π*) is intermediate in size, and so are the participation of the π* orbital and the tilt angle. The molecular and electronic structures of the Ir complex show that the participation of the thiophene π* orbital in the bonding depends not only on the nature of the transition metal, but also on the nature of the other ligands bound to the metal, since without the donor ligands on the Ir^{3+} center, we would expect E(M-π*) in this complex to be considerably larger.

In the η^1–S bound complexes (just as in the η^5 complexes), the π acceptor ability of thiophene can and does become important under certain conditions. The orbital structures of the η^1 complexes suggest that increasing the electron density on the metal (thus increasing back donation to thiophene and weakening of the C—S bond through population of the π* orbital) could provide a pathway to activating the thiophene ring in S-bound complexes. This observation is consistent with the identification of an S-bound intermediate as the precursor to ring opened complexes such as $Cp^*(PMe_3)Rh[C,S\text{-}(SC_4H_4)]$, where it is clear that oxidative addition to the electron rich metal center occurs in the bond insertion reaction [13]. Our preliminary calculations on a model five coordinate S-bound intermediate for this reaction indicate, not surprisingly, that occupation of the thiophene π^* orbital also plays an important role in this oxidative addition process.

Metal inserted complexes

Ring-opened or metal-inserted complexes result when a transition metal center inserts, via an oxidative addition reaction, into a C—S bond of thiophene or a derivative. Examples of several such complexes are illustrated in Fig. 4. These complexes are of particular interest because some (such as $(PEt_3)_2Pt[C,S\text{-}(SC_{12}H_8)]$ and $(triphos)Ir[C,S\text{-}(SC_8H_6)]^+$) undergo reactions that lead to sulfur removal from the metallathiacycle. Although these specific platinum and iridium complexes exhibit the ability to desulfurize thiophenic molecules, many similar transition metal inserted thiophene complexes have not shown such potential as HDS models. This is somewhat surprising, given the similarities of these complexes (Fig. 4). The differences in reactivity among very similar complexes prompted us to examine the electronic structures of a number of these complexes [6].

The complexes can be divided into two distinct groups. The first group includes $Cp^*Ir[C,S\text{-}2,5\text{-}Me_2(SC_4H_2)]$ and $(triphos)Ir[C,S\text{-}(SC_8H_6)]^+$. These complexes are characterized by a planar metallacycle ring and are formally 16-electron complexes. The equivalent C—C bond lengths around the ring suggest that metal orbitals participate in delocalized π bonding and that it is probably appropriate to view the metallacycle rings as 'iridathiabenzenes'. The second group, which includes all of the other complexes illustrated in Fig. 4, are formally 18 electron complexes (or in the Pt complex a stable 16 electron square planar complex).

It is convenient to view the bonding in all of the ring opened complexes in terms of the interactions between metal based orbitals and the orbitals of a ring opened thiophenic fragment. The relevant orbitals of the opened benzothiophene fragment are illustrated in both Figs 5 and 6. (Although not shown, the corresponding orbitals in a ring opened thiophene fragment are very similar.) The HOMO (Highest Occupied Molecular Orbital) in the fragment is a π orbital perpendicular to the plane of the five-membered ring system. A distinctive characteristic of the

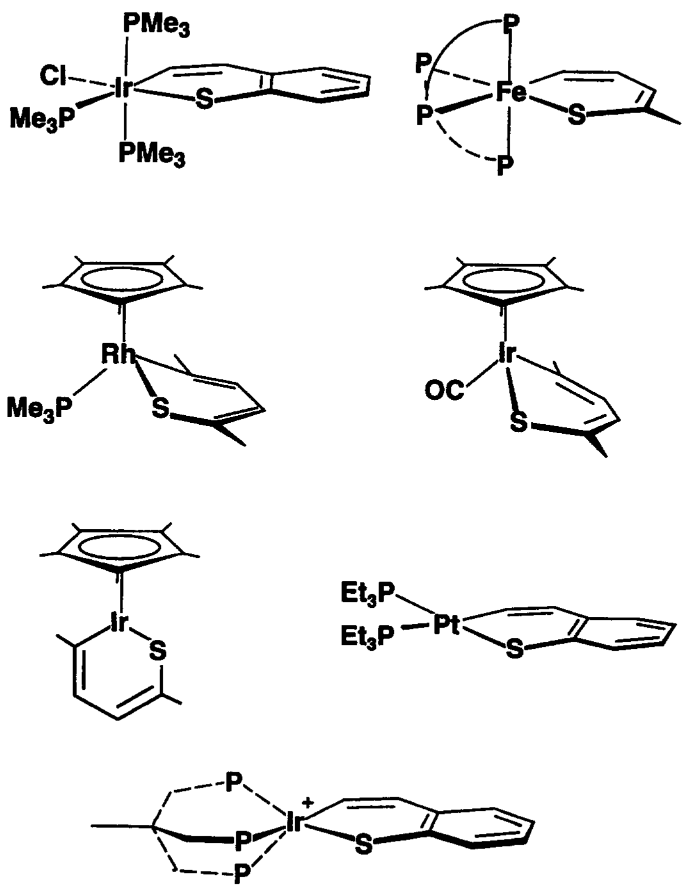

Fig. 4. Structures of metal-inserted thiophene and benzothiophene complexes.

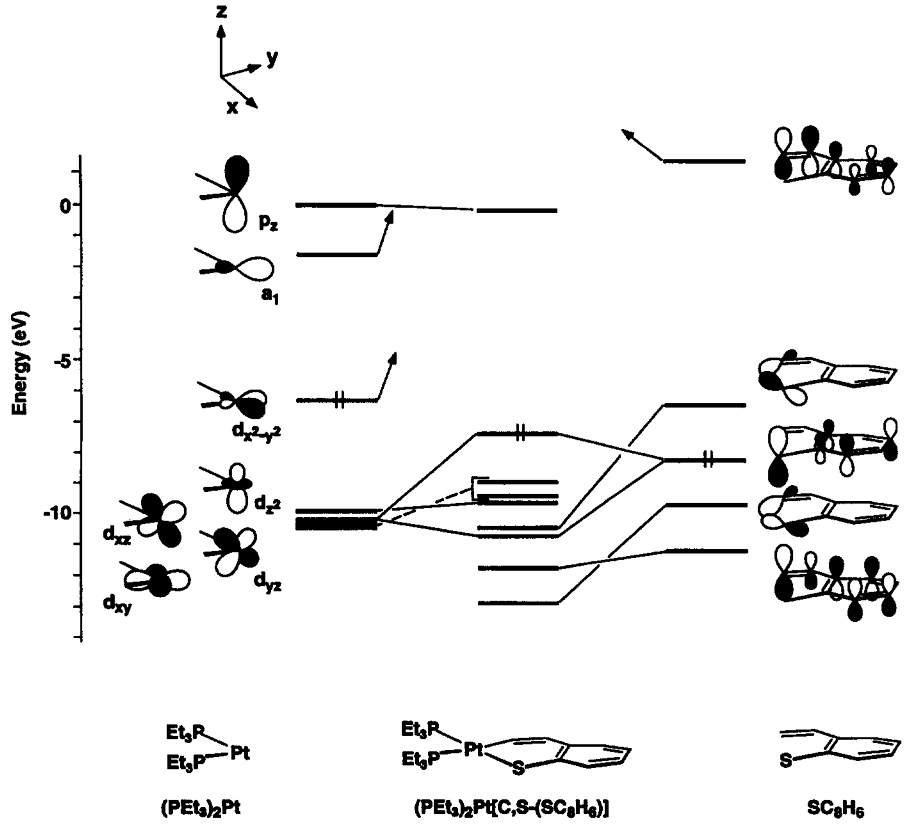

Fig. 5. Calculated energy level diagrams for $(PEt_3)_2Pt[C,S\text{-}(SC_8H_6)]$ and for the $(PEt_3)_2Pt$ and opened benzothiophene fragments.

HOMO is the large percentage of the orbital, 50–65%, centered on the sulfur. The SHOMO (Second Highest Occupied Molecular Orbital) and the LUMO (Lowest Unoccupied Molecular Orbital) are both σ orbitals, bonding and antibonding, respectively, with respect to the opened C—S bond. In these orbitals, electron density resides on both the sulfur and carbon and is directed at the inserting transition metal. The third highest energy occupied and the second lowest unoccupied molecular orbitals are both π orbitals perpendicular to the ring systems. For the opened benzothiophene fragment, the electron density on both of these π orbitals is localized on the α-carbon. For the thiophene fragments, equivalent electron density resides on both the sulfur and the carbon in these two orbitals.

We have calculated the orbital structures of all of the complexes shown in Fig. 4, but our discussion here will center around $(PEt_3)_2Pt[C,S\text{-}(SC_{12}H_8)]$ and $(triphos)Ir[C,S\text{-}(SC_8H_6)]^+$. The bonding in these two complexes illustrates the features of both the 'saturated' and 'unsaturated' complexes and is of particular interest since both complexes undergo reactions leading to sulfur removal. The calculated energy level diagrams for $(PEt_3)_2Pt[C,S\text{-}(SC_8H_6)]$ and for the $(PEt_3)_2Pt$ and open benzothiophene fragments are shown in Fig. 5. The d^8 platinum inserted benzothiophene complex is essentially square planar (despite a slight umbrella effect and L—M—L bond angle distortions), with the benzothiophene occupying two coordination sites and two donor phosphine ligands occupying the other two opposing coordination sites. The metal orbitals involved in bonding with the opened benzothiophene are σ orbitals formed from the mixing of two metal orbitals. Specifically, the a_1 and $d_{x^2-y^2}$ molecular orbitals mix together upon complex formation to form two metal orbitals; one is directed at the incoming sulfur and the other at the α-carbon. Bond formation thus results from the donation of electron density from the metal HOMO and benzothiophene SHOMO into the benzothiophene LUMO and the metal LUMO, respectively. A net transfer of a pair of electrons from the metal to the benzothiophene occurs since the pair of electrons which in the d^{10} fragment occupied the $d_{x^2-y^2}$ metal orbital now resides in a lower energy metal-benzothiophene σ-bonding orbital centered primarily on the ligand. The transfer of electron density is also reflected in a more positive charge on the metal after insertion (-0.79 in the d^{10} fragment versus -0.38 after insertion). Sigma bond formation using the SHOMO and LUMO ligand orbitals and the HOMO and LUMO metal fragment orbitals is a feature of all of the 18-electron or 'saturated' metal-inserted complexes we have studied. The formation of these bonds is always accompanied by the transfer of a pair of electrons from metal to ligand based orbitals

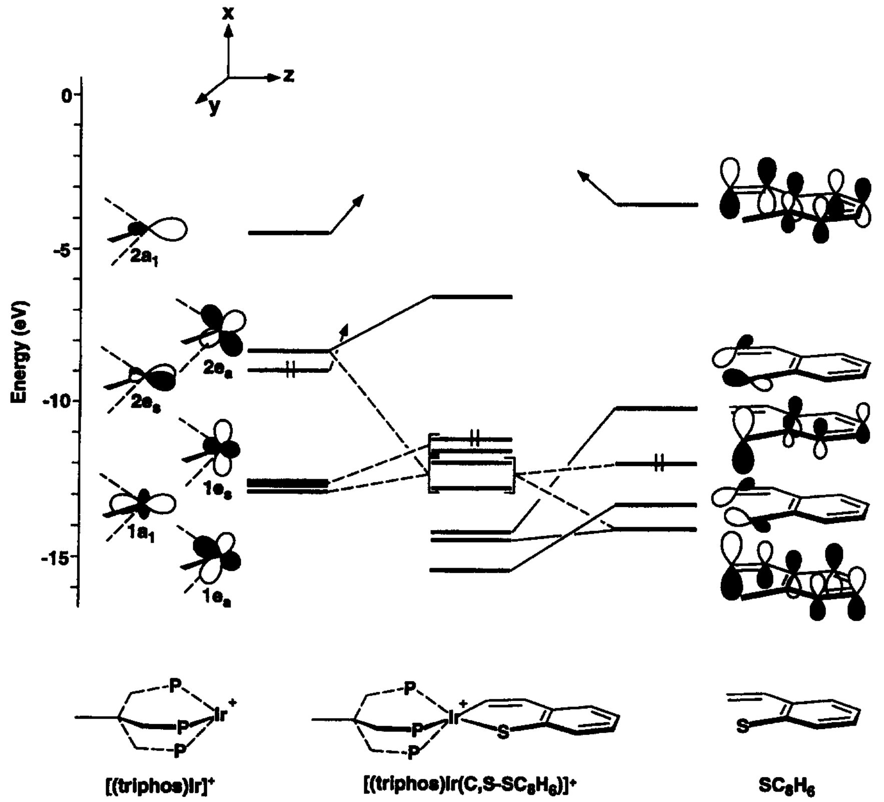

Fig. 6. Calculated energy level diagrams for (triphos)Ir[C,S-$(SC_8H_6)]^+$ and for the $[(triphos)Ir]^+$ and opened benzothiophene fragments.

and a more positive charge on the metal center. The residual charge on the metal after insertion correlates with the number of donor ligands and their ability to donate electron density to the metal. These charges vary from negative, as in the Pt complex, to positive, as in Cp*Ir(CO)[C,S-2,5-$Me_2(SC_4H_2)$] where the calculated charge for Ir is +0.78.

The orbital diagram in Fig. 5 exhibits one particularly striking feature; the HOMO of the Pt complex is a metal-ligand antibonding orbital centered primarily on the sulfur of the benzothiophene. This comes about because the filled metal d_{xz} orbital interacts strongly with the HOMO of the 'opened' benzothiophene. This interaction results in a filled bonding/antibonding set of orbitals, and it is the antibonding molecular orbital of the set which forms the HOMO in the complex. The HOMO is thus primarily ligand based and, furthermore, predominantly sulfur in character. The HOMO is essentially a lone pair of electrons isolated on the sulfur. This filled-filled interaction which results in an antibonding, sulfur-based HOMO is a characteristic of most of the 'saturated' metal inserted complexes.

The high sulfur character of the HOMO provides an explanation for at least some of the reactivity of these Pt complexes. Maitlis and coworkers, for example, have shown that protonation of the analogous dibenzothiophene platinum complex produces 2-phenylthiophenol [17]. Our results for the benzothiophene complex suggest that such a reaction probably occurs *via* initial attack at the thiophenic sulfur; that is, electrophilic attack at the sulfur is expected due to the high energy, sulfur-based HOMO of the complex and the negatively charged sulfur atom. The similar sulfur character of the HOMO's in $Cl(PMe_3)_3$Ir[C,S-(SC_8H_6)], Cp*(PMe_3)Rh[C,S-2,5-$Me_2(SC_4H_4)$], and Cp*Ir(CO)[C,S-2,5-$Me_2(SC_4H_2)$] suggests that these complexes should also be susceptible to electrophilic attack at the sulfur.

Bianchini and coworkers have also demonstrated selective attack of Me^+ and H^+ at sulfur for the 18-electron hydride species, (triphos)Ir(H)[C,S-(SC_8H_6)] and its thiophene and dibenzothiophene analogs [31]. Although the crystal structure of this complex has not been determined, similarities in ligands and coordination geometry suggest that both the molecular and electronic structures of (triphos)Ir(H)[C,S-(SC_8H_6)] and its analogs should closely resemble those of other d^6 octahedral complexes such as $Cl(PMe_3)_3$Ir[C,S-(SC_8H_6)]. Thus we expect that the nucleophilicity of the sulfur in these hydride complexes also arises from the presence of an antibonding, sulfur based HOMO.

A feature of the Pt complex which is *not* common to all of the saturated complexes is the presence of a metal-based LUMO, and this feature is probably responsible for the observed reactivity of the metal center. Unlike other saturated complexes, $(PEt_3)_2Pt[C,S-(SC_{12}H_8)]$ and the analogous square planar thiophene and benzothiophene complexes can be cleaved by hydridic reagents to yield styrene, C_4 hydrocarbons, and biphenyl, respectively. Hydridic attack on $(PEt_3)_2Pt[C,S-(SC_8H_6)]$ has been suggested to occur *via* initial H–X oxidative addition to the metal. Of the saturated complexes we studied, only $(PEt_3)_2Pt[C,S-(SC_8H_6)]$ exhibits a low energy metal-based LUMO and an open coordination site on the metal. In addition, the metal center carries a relatively high negative charge. The readily accessible metal-based LUMO and the electron rich metal center are certainly consistent with the proposed oxidative addition.

The orbital structures of the two 'unsaturated' complexes are quite different from those calculated for the saturated complexes. The energy level diagrams for $(triphos)Ir[C,S-(SC_8H_6)]^+$ and for the $[(triphos)Ir]^+$ and opened benzothiophene fragments are shown in Fig. 6. The electronic structures of this complex and of the similar complex synthesized earlier by Angelici exhibit many of the same features. Four metal orbitals (the occupied $1a_1$, $1e_s$, and $2e_s$, and the unoccupied $2a_1$) participate in σ interactions with the benzothiophene. Combinations of these metal orbitals form two σ bonding orbitals with the opened benzothiophene fragment. In addition to the two bonding orbitals, two nearly nonbonding σ orbitals which are primarily metal based form the SHOMO and HOMO of the complex. (Two unoccupied σ-antibonding orbitals occur at much higher energy.)

The π orbital interactions in this complex (and in the similar $Cp^*Ir[C,S-2,5-Me_2(SC_4H_2)]$) are unique. In the saturated complexes, the important π interaction involves the thiophene HOMO and a filled 'π' metal orbital. The product is a bonding/antibonding pair of orbitals; the antibonding partner is the HOMO of the complex. The only filled metal 'π' orbital in the $[(triphos)Ir]^+$ fragment ($1e_a$), however, is not able to interact with the benzothiophene HOMO because this HOMO has no electron density on the α-carbon. The only other metal 'π' orbital available for interaction with the benzothiophene HOMO is the $2e_a$ fragment LUMO. This interaction produces both a π molecular orbital which is slightly bonding between the metal and the sulfur, and an antibonding counterpart. Because this π interaction occurs between an occupied ligand orbital and an unoccupied metal orbital, the antibonding partner is the LUMO of the complex. In all of the saturated complexes, π bonding between the metal and the thiophene HOMO is cancelled out by a filled antibonding partner. In the unsaturated complexes, since the π antibonding molecular orbital is unoccupied, the metal-ligand bonding is not solely σ in character. There is now a π component, which serves to donate electron density from the ligand to the metal.

As in the saturated complexes, the insertion of iridium into the C—S bond of the benzothiophene can be viewed as an oxidative addition. Whereas oxidation of the metals in the saturated complexes results in significant changes in metal charge, the oxidation of the metal centers in the unsaturated complexes has little effect on the metal charges. (Calculated Ir charges in the $[(triphos)Ir]^+$ fragment and $(triphos)Ir[C,S-(SC_8H_6)]^+$ are -0.64 and -0.54, respectively.) In both $(triphos)Ir[C,S-(SC_8H_6)]^+$ and $Cp^*Ir[C,S-2,5-Me_2(SC_4H_2)]$ participation of the metal orbitals in the π system of the benzothiophene forces electron density back onto the metal, and the orbital structures of both complexes provide evidence for the π delocalization. Specifically, although the HOMO and SHOMO in both complexes are localized on the metal, the charge density in the third and fourth highest energy occupied molecular orbitals is distributed much more evenly between the metal and ligand π orbitals. The π delocalization in these complexes is consistent with the equivalent C—C bond distances observed in the metallathiacycle ring.

Like the square planar platinum inserted compound, the LUMO's of $(triphos)Ir[C,S-(SC_8H_6)]^+$ and $Cp^*Ir[C,S-2,5-Me_2(SC_4H_2)$ are not only metal-based, but are also accessible, in terms of having an open coordination site (this coordination site is somewhat hindered in $(triphos)Ir[C,S-(SC_8H_6)]^+$ due to the very bulky triphos ligand), to nucleophilic attack. Angelici has shown that nucleophiles such as PR_3 or CO readily add to the metal center in $Cp^*Ir[C,S-2,5-Me_2(SC_4H_2)$ [32], and Bianchini has demonstrated hydride attack at the metal in $(triphos)Ir[C,S-(SC_8H_6]^+$ [16,33]. While nucleophilic attack at the metal centers in these complexes can be related simply to the character of the LUMO and the availability of an open coordination site, differences in the further reactivity of the two complexes are probably related to both the large steric bulk and the strong donor ability of the triphos ligand. The Ir charges in $(triphos)Ir[C,S-(SC_8H_6)]^+$ and $Cp^*Ir[C,S-2,5-Me_2(SC_4H_2)]$ are -0.54 and $+0.51$, respectively. While the orbital structures of the two complexes are similar, only the triphos complex exhibits an electron rich metal center.

Finally, the orbital structure of the unsaturated complexes suggests that the sulfur center in these complexes should not be susceptible to electrophilic attack. The sulfur π orbital which is localized in the HOMO of the saturated complexes is now involved in delocalized metal-ligand bonding. This difference in orbital character is consistent with the fact that H^+ does not attack the sulfur atom in $(triphos)Ir[C,S-(SC_8H_6)]^+$, but does attack the sulfur atom in the 18-electron hydride species, $(triphos)Ir(H)[C,S-(SC_8H_6)]$ (see above).

Metal–sulfur clusters

While much of the work aimed at developing molecular HDS models has approached the problem by

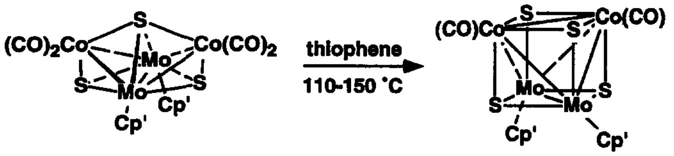

(1)

studying the binding and activation of thiophenic molecules in complexes containing a single metal center, the Curtis group has utilized bimetallic metal-sulfur clusters to model the HDS process [34,35]. In a series of particularly intriguing reactions, Curtis has shown that the 'butterfly' cluster $(Cp')_2Mo_2Co_2S_3(CO)_4$ ($Cp' = CH_3C_5H_4$) is able to remove sulfur directly from thiophene (Eq. 1) [22,23]. This reaction produces a cubane cluster, $(Cp')_2Mo_2Co_2S_4(CO)_2$ [36].

Although the mechanism for the reaction of thiophene with the butterfly cluster is not understood, reactions of the cluster with other nucleophiles indicate that initial binding of the thiophene to the cluster probably occurs at one of the Co centers. We carried out molecular orbital calculations on the butterfly, the cubane, and several related clusters in order to try to better understand how thiophene might bind to and react with the butterfly cluster [37]. The bonding in the cubane is very similar to that in analogous clusters which we studied earlier [38,39]. We found previously that it is convenient to view the formation of the metal-metal bonds in the cubane clusters in terms of metal–sulfur-ligand fragment orbitals. In the terminology of ref. [39], the $(Cp')_2Mo_2Co_2S_4(CO)_2$ cubane falls into the general classification of a cluster of formula $M_2M'_2S_4Cp_2L'_2$, where the two M(Mo) centers and two M′(Co) centers have 'octahedral' and 'tetrahedral' coordination geometry, respectively. The Mo–ligand interactions split the Mo orbitals into t_{2g} and e_g groups, while the Co–ligand interactions split the Co orbitals into e and t_2 groups. These metal-based orbitals are used in the formation of metal–metal bonds in the cluster. A qualitative bonding scheme for the metal-based orbitals in a cluster of this type is shown in Fig. 7. (The calculated orbital structure of $(Cp')_2Mo_2Co_2S_4(CO)_2$ shows these features.) Metal–metal bonding utilizes the t_{2g} and t_2 orbitals, while the e_g and e orbitals remain nonbonding (in terms of metal–metal bond formation). This leads to four groups of metal-based cluster orbitals. The lowest energy group arises from the two sets of Co e orbitals. These orbitals are metal–metal *nonbonding*. The highest energy group arises from the two sets of Mo e_g orbitals. These orbitals are also metal–metal *nonbonding*. The two groups of intermediate energy are combinations of the two sets of Mo t_{2g} orbitals and the two sets of Co t_2 orbitals. These 12 metal-based orbitals combine to form six metal–metal bonding and six metal–metal antibonding orbitals. Given this orbital structure, a cluster having 20 metal-based electrons will have six metal–metal bonds. Eight electrons will occupy the four lower energy Co-based non-bonding orbitals, while the remaining 12 electrons will occupy the six metal–metal bonding orbitals. This is exactly what is found for the cluster $(Cp')_2Mo_2Co_2S_4(CO)_2$, where 20 metal electrons can be associated with two Mo^{5+} (d^1) and two Co^0 (d^9) centers.

Our molecular orbital calculations for the butterfly cluster showed that it is also useful to view the metal–metal bonding in this cluster in terms of 'octahedral' Mo fragments and 'tetrahedral' Co fragments, although now the Co is bound to two CO and two S^{2-} ligands instead of one CO and three S^{2-} ligands. The calculated energy level diagrams for $(Cp')_2Mo_2Co_2S_3(CO)_4$ and for the 'octahedral' Mo and 'tetrahedral' Co fragments are shown in Fig. 8. The diagram is in many ways similar to the qualitative diagram for the cubane cluster. The groups of Mo t_{2g} and e_g and Co t_2 and e_g orbitals are apparent for the two fragments, and the cluster metal-based orbitals separate into high and low energy groups of nonbonding orbitals, and intermediate groups of bonding and antibonding orbitals. Further examination of the diagram reveals, however, that the bonding (b) and antibonding (ab) groups of orbitals include seven and five orbitals, respectively (not six and six as in the cubane). Only five of the 'bonding' cluster orbitals are actually bonding between the metals. These arise from combinations of all of the Mo t_{2g} orbitals and the a_1 and b_1 orbitals from the Co t_2 sets of orbitals. These combinations lead to five metal–metal bonding and five metal–metal antibonding orbitals. Occupation of the five bonding orbitals is consistent with the five metal–metal bonds in the cluster. The other two orbitals (orbitals 71 and 74 in Fig. 8) are combinations of the b_2 orbitals from the two Co fragments. These orbitals, which lie in the plane of the two Co's and three S's, are not oriented properly to interact with the Mo centers. Although the two cluster orbitals are plus (bonding) and minus (antibonding) combinations of the Co b_2 orbitals, the distance between the two Co centers is far too large for any Co–Co interaction. If the cluster were a tetrahedron (i.e. if the top sulfur were removed and the two Co's pushed together), the two fragment b_2 orbitals would overlap, and the two cluster orbitals would be truly bonding and antibonding and well separated in energy. In the butterfly cluster, however, where the two Co's are too far apart to interact, these cluster orbitals are nonbonding with respect to metal–metal interactions and lie close together in energy.

Comparisons of the orbital structures and charge distributions in the butterfly and cubane allow us to point out several substantial differences in the clusters.

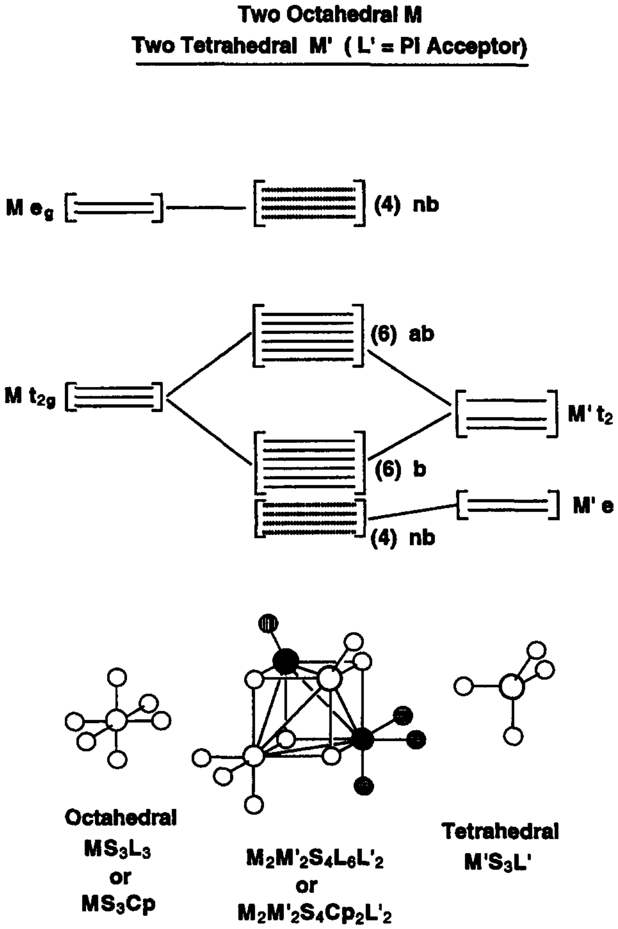

Fig. 7. Qualitative energy level scheme for the metal-based cluster orbitals in a heterometallic $M_2M'_2S_4L_6L'_2$ or $M_2M'_2S_4Cp_2L'_2$ cluster containing two octahedral metals and two tetrahedral metals. L′ is a pi acceptor ligand. (Ref. [39]).

Firstly, 22 and 20 metal electrons occupy the metal-based cluster orbitals in the butterfly and cubane, respectively. The two extra electrons are associated with the Co centers. In fact, the presence of the two additional occupied nonbonding Co-based orbitals (71 and 74) in the butterfly means that an extra nonbonding pair of electrons is associated with each Co center in this cluster. This excess electron density on the Co centers is reflected in the differences in calculated metal charges in the two clusters. The Co charges are -0.15 and -0.01 in the butterfly and cubane, respectively. Each Co center is more negative by -0.14 in the butterfly, despite the fact each Co is coordinated to two π-acceptor and two donor ligands in the butterfly and one π-acceptor and three donor ligands in the cubane. The Mo charges are nearly constant in the two clusters: $+0.87$ and $+0.90$ in the butterfly and cubane respectively. While discussions by Curtis *et al.* have made it clear that the butterfly is not 'electron precise' [40,41], these calculations make it clear not only that the cluster has excess electron density but also that the extra electrons are associated with the Co centers.

The reaction (Eq. 1) in which a sulfur atom adds to the cluster to form the cubane is accompanied by the transfer of two electrons from the metal framework to the added sulfur. That is, the metal framework is oxidized. Comparisons of the orbitals in the two clusters make it clear that it is actually the Co centers which are oxidized. Formation of the new Co—Co bond in the cubane converts the 'nonbonding' Co based butterfly orbitals (71 and 74) to orbitals which now are truly bonding and antibonding. The bonding orbital remains occupied, while the antibonding orbital is destabilized and, with two less electrons in the metal framework, unoccupied. Thus oxidation of the metal framework removes two electrons from an orbital which in the butterfly is localized on the Co centers; the Co centers are oxidized. Although assigning oxidation states in these large clusters is always done with some trepidation, we believe that it is most appropriate to view the electron rich Co centers in the butterfly as Co^{1-}. These centers are each oxidized to Co^0 in the butterfly. The Mo centers then remain Mo^{5+} in both clusters. These assignments are consistent with the make-up and occupations of the metal-based cluster orbitals and the calculated charges.

The assignment of this negative oxidation state to

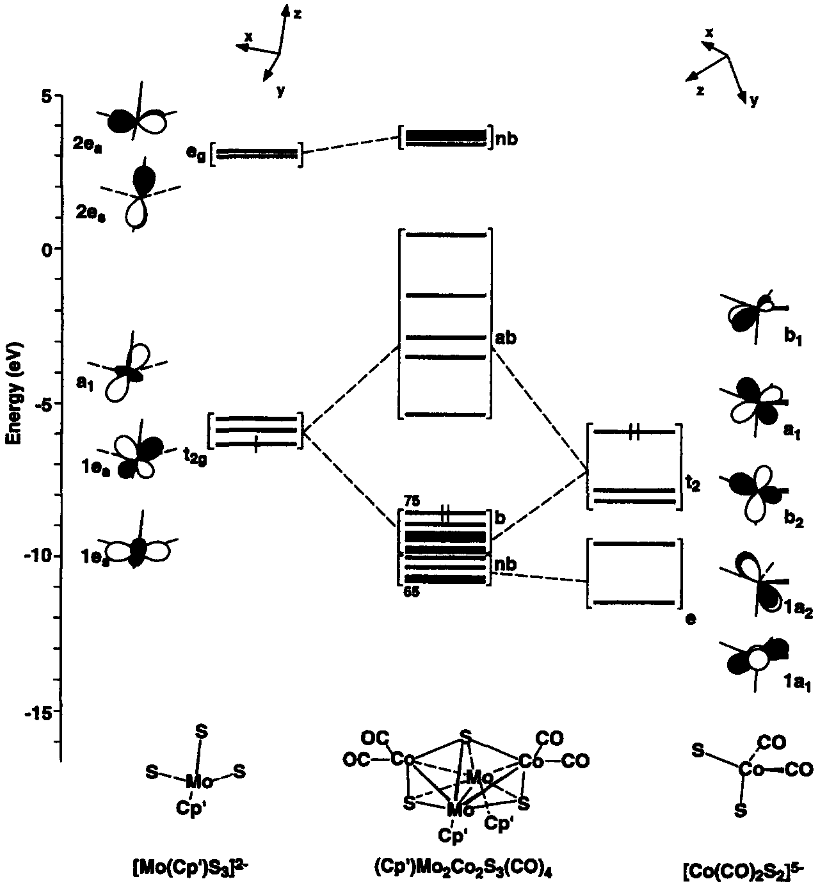

Fig. 8. Calculated energy level diagrams for $(Cp')_2Mo_2Co_2S_3(CO)_4$ and for the component $[MoCp'S_3]^{2-}$ and $[CoS_2(CO)_2]^{5-}$ fragments.

the Co center in the butterfly at first appears to be inconsistent with the fact that this Co center is susceptible to nucleophilic attack. Examination of the character of the LUMO in the butterfly shows, however, how a nucleophile such as thiophene may both bind and react at the Co center in the butterfly. While the LUMO is antibonding between the Co's and Mo's and has both Co and Mo character, the Co character (illustrated in **1**) is the important feature. Since the LUMO is also strongly antibonding between the Co's and the sulfurs below the Co's, the Co electron density in this orbital is concentrated in the regions opposite these sulfurs. Thus the LUMO resembles an unoccupied combination of large Co σ orbitals which are accessible to an attacking nucleophile. The orbital structure of the butterfly cluster thus suggests that nucleophilic attack at a Co center is possible because of the nature of the LUMO. Binding at this site must be followed by what is essentially an oxidative addition involving both Co centers. It is intriguing that although the mechanisms for desulfurization of thiophene in this cluster and in the ring-inserted complexes discussed in the previous sections may be different, they both appear to involve oxidative addition of thiophene to an electron rich, late transition metal center. It is not clear, however, why in the butterfly cluster this reaction proceeds rapidly, with no identifiable intermediate, to desulfurize the thiophene ring, while in the simple metal complexes the reaction results in metal insertion into the thiophene ring. Does the desulfurization reaction of thiophene with the butterfly cluster also involve a ring inserted intermediate, or does the presence of *two* electron rich metal centers provide another facile pathway to desulfurization?

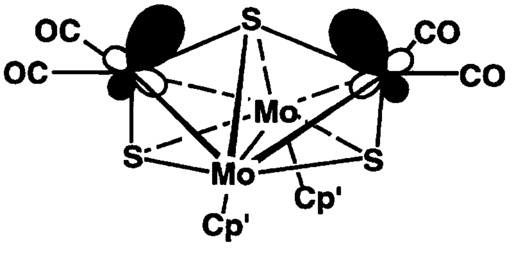

(1)

Although no intermediate has been identified in the desulfurization reaction, Curtis *et al.* have attempted to better understand the desulfurization reaction by reacting the butterfly with other nucleophiles such as

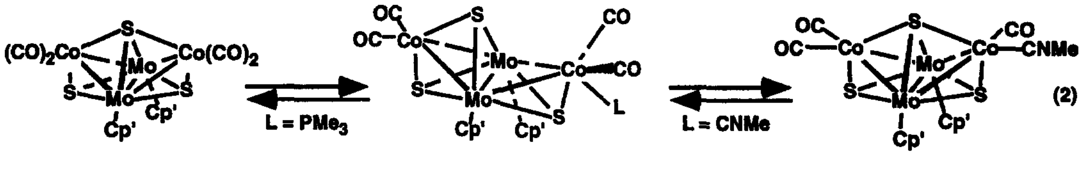

(2)

P(Me$_3$) and CNMe. They find that while reactions of phosphine or isocyanide with the butterfly lead to formation of 'intermediate' clusters, both 'intermediates' revert back to a butterfly cluster (Eq. 2). CNMe replaces CO to form a substituted butterfly cluster while PMe$_3$ is displaced to reform the original butterfly cluster [40,41]. We have carried out molecular orbital calculations on both the intermediate and substituted clusters, and our results indicate that the donor and/or acceptor properties of the added ligand determine whether CO or the new ligand is displaced. As described above, the two π acceptor CO ligands serve to stabilize the electron rich Co centers in the butterfly cluster. Although CNMe is not as strong a π acceptor as CO, it does serve as an acceptor and can thus replace CO. It is unfavorable, however, to replace an acceptor CO with a donor PMe$_3$, since the reduced Co center requires the acceptor ligand for stability. While these results help explain the behavior of intermediates that incorporate PMe$_3$ or CNMe, they do not explain why an intermediate is not observed when thiophene reacts with the butterfly or why desulfurization is observed. Presumably, coordination of a donor such as a thiol or thiophene should be similar to coordination of a phosphine. Why do they behave so differently? Again, this is a question that we cannot yet answer. We hope that calculations modeling reactions and possible intermediates involving thiols will help us answer several such important questions.

Other cubane clusters

We have also recently begun to study a group of cubane clusters characterized by an Mo$_3$NiS$_4$ or Mo$_3$PdS$_4$ core. There has been considerable discussion in the literature regarding the assignment of oxidation states in these clusters [42,43]. In addition, the unusual reactivity of the Ni or Pd center in these clusters has prompted suggestions that these clusters may also provide good models for HDS catalysts [44]. The results of our calculations indicate that Ni is present in the clusters as Ni^0 (not Ni^{2+} as has been suggested) but that the Ni electron density is strongly delocalized throughout the metal–metal bonding framework. This delocalization is even greater for Pd. Although we do not believe that Ni or Pd is formally oxidized in these clusters, it is clear that the presence of one rather than two heterometal centers (as in the cubane discussed above) has a substantial effect on the electronic properties of the heterometal. In particular, the metal charge delocalization reduces the electron density associated with Ni or Pd and weakens some metal-ligand bonds. Our calculations also suggest that varying the ligands on the Mo centers has a considerable effect on the Ni or Pd center.This in turn suggests that the reactivity at the Ni or Pd center might be 'tuned' by varying the ligands on the Mo centers. This is an area that both we and experimental groups will continue to study.

SUMMARY

The electronic structures of η^5- and η^1-thiophene complexes reveal that while donation from the thiophene orbitals to the metal is the major contributor to metal-ligand bonding, the vacant thiophene π^* orbital can and does interact with the metal orbitals. π Back-donation becomes measurable, particularly for the larger 4d and 5d metals, when the metal orbitals lie sufficiently close in energy to the ligand π^* orbital. Thus π back-donation should become most important when thiophene is bound to a 4d or 5d metal that is in a low oxidation state and/or is bound to other strong *donor* ligands. This increases the metal–sulfur orbital overlap, increases the electron density on the metal, and decreases the energy separation between the occupied metal π orbital(s) and the unoccupied thiophene π^* orbital. Maximizing the π back-donation would weaken the C—S bond and could provide a pathway to activation of this C—S bond.

The electronic structures of the metal-inserted complexes vary with metal center, coordination geometry, and the donor ability of the other ligands. The most notable differences are found in the frontier orbital structures of the saturated and unsaturated metal-inserted complexes. The 18-electron or saturated complexes are generally characterized by a sulfur based HOMO. The character of this orbital is consistent with the observed susceptibility to electrophilic attack of the sulfur in both (PEt$_3$)$_2$Pt[C,S-(SC$_8$H$_6$)] and (triphos)Ir(H)[C,S-(SC$_8$H$_6$)] and suggests that the sulfur in other similar complexes should be equally reactive. Reactivity at the metal center is observed only in the coordinatively unsaturated Pt complex, and this is also consistent with the orbital structures of the complexes. Only the coordinatively unsaturated platinum complex displays both an accessible unoccupied low-lying metal orbital *and* an electron rich metal center. These features are consistent with reactivity at the metal center proceeding *via* an oxidative addition.

The unsaturated complexes exhibit a metal-based HOMO *and* a metal-based LUMO. The sulfur π electrons which in the saturated complexes are localized in the HOMO are now involved in delocalized metal-ligand bonding. Thus the sulfur center in these complexes should not be susceptible to electrophilic attack. The LUMO's are both metal-based and accessible (since these complexes are coordinatively unsaturated), and this feature provides an explanation for the susceptibility of the metal centers to nucleophilic attack. Differences in further reactivity probably stem from both charge and steric effects.

Comparisons of the electronic structures of the butterfly and cubane clusters, $(Cp')_2Mo_2Co_2S_3(CO)_4$ and $(Cp')_2Mo_2Co_2S_4(CO)_2$, respectively, indicate that the mechanism of sulfur abstraction from thiophene by the butterfly cluster [36] may share features with the mechanisms of sulfur abstractions involving the ring-opened complexes. Specifically, the substantial Co character of the LUMO in the butterfly and the clearly defined oxidation of the Co centers in going from the butterfly to the cubane are consistent with initial binding of the thiophene at a Co center followed by an oxidative addition. The fact that sulfur removal occurs rapidly with no observable intermediate, however, makes it attractive to speculate that it is the presence of two electron-rich Co centers which provides the facile pathway to desulfurization.

Both the ability of complexes and clusters incorporating electron rich, low oxidation state late transition metal centers to activate C—S bonds (and in some cases to completely desulfurize thiophenic ligands) and the oxidative additions always involved in these reactions make it attractive to speculate even further that the chemistry observed in these reactions may truly provide a model for the heterogeneous HDS reactions. The heterogeneous reactions occur readily over late transition metal sulfides (e.g. RuS_2, Rh_2S_3). Under the reducing atmosphere of high H_2 pressures, the surfaces of these sulfides undoubtedly exhibit coordinatively unsaturated reduced metal sites. A redox HDS mechanism involving binding of thiophene at one of these electron rich sites, oxidative addition, sulfur removal and reduction of the metal is not unreasonable.

In summary, although we still do not understand the mechanism of heterogeneous HDS, homogeneous models have begun to provide possible reaction pathways, and electronic structure calculations have begun to provide an understanding of the role of particular metal centers, ancillary ligands, coordination geometry (around the metal), and coordination mode of the thiophenic ligand in these reaction pathways.

Acknowledgements—Students and colleagues who carried out much of the work described here are cited in the references. Their work is greatly appreciated. Financial support by the National Science Foundation (Grant CHE94-21784) and by NSF and DOE EPSCoR is gratefully acknowledged.

REFERENCES

1. Angelici, R. J., *Coord. Chem. Rev.* 1990, **105,** 61.
2. Rauchfuss, T. B., *Prog. Inorg. Chem.* 1991, **39,** 251.
3. Bianchini, C. and Meli, A., *J. Chem. Soc., Dalton Trans.* 1996, 801
4. Harris, S., *Organometallics* 1994, **13,** 2628.
5. Carter, K. and Harris, S., Manuscript in preparation.
6. Palmer, M., Carter, K. and Harris, S., *Organometallics*, in press.
7. Lesch, D. A., Richardson, Jr. J. W., Jacobson, R. A. and Angelici, R. J., *J. Am. Chem. Soc.* 1984, **106,** 2901.
8. Spies, G. H. and Angelici, R. J., *Organometallics* 1987, **6,** 1897.
9. Goodrich, J. D., Nickias, P. N. and Selegue, J. P., *Inorg. Chem.* 1987, **26,** 3424.
10. Choi, M.-G. and Angelici, R. J., *Organometallics* 1991, **10,** 2436.
11. Benson, J. W. and Angelici, R. J., *Organometallics* 1992, **11,** 922.
12. Rao, K. M., Day, C. L., Jacobson, R. A. and Angelici, R. J., *Inorg. Chem.* 1991, **30,** 5046.
13. Jones, W. D. and Dong, L., *J. Am. Chem. Soc.* 1991, **113,** 559.
14. Selnau, H. E. and Merola, J. S., *Organometallics* 1993, **12,** 1583.
15. Bianchini, C., Meli, A., Peruzzini, M., Vizza, F., Frediani, P., Herrera, V. and Sánchez-Delgado, R. A., *J. Am. Chem. Soc.* 1993, **115,** 7505.
16. Bianchini, C., Meli, A., Peruzzini, M., Vizza, F., Moneti, S., Herrera, V. and Sánchez-Delgado, R. A., *J. Am. Chem. Soc.* 1994, **116,** 4370.
17. Garcia, J. J. and Maitlis, P. M., *J. Am. Chem. Soc.* 1993, **115,** 12200.
18. Chen, J., Daniels, L. M. and Angelici, R. J., *J. Am. Chem. Soc.* 1990, **112,** 199.
19. Buys, I. E., Field, L. D., Hambley, T. W. and McQueen, A. E. D., *J. Chem. Soc., Chem. Commun.* 1994, 557.
20. Bianchini, C., Jimenez, M. V., Meli, A., Moneti, S., Vizza, F., Herrera, V. and Sánchez-Delgado, R., *Organometallics* 1995, **14,** 2342.
21. Garcia, J. J., Mann, B. E., Adams, H., Bailey, N. A. and Maitlis, P. M., *J. Am. Chem. Soc.* 1995, **117,** 2179.
22. Riaz, U., Curnow, O. and Curtis, M. D., *J. Am. Chem. Soc.* 1991, **113,** 1416.
23. Riaz, U., Curnow, O. J. and Curtis, M. D., *J. Am. Chem. Soc.* 1994, **116,** 4357.
24. Hall, M. B. and Fenske, R. F., *Inorg. Chem.* 1972, **11,** 768.
25. Mulliken, R. S., *J. Chem. Phys.* 1955, **23,** 1833.
26. Herman, F. and Skillman, S., *Atomic Structure Calculations*, Chapter Prentice-Hall, Englewood Cliffs, NJ (1963).
27. Bursten, B. E., Jensen, J. R. and Fenske, R. F., *J. Chem. Phys.* 1978, **68,** 3320.
28. Clementi, E., *J. Chem. Phys.* 1964, **40,** 1944.
29. Lockemeyer, J. R., Rauchfuss, T. B., Rheingold, A. L. and Wilson, S. R., *J. Am. Chem. Soc.* 1989, **111,** 8828.
30. Ganja, E. A., Rauchfuss, T. B. and Stern, C. L., *Organometallics* 1991, **10,** 270.
31. Bianchini, C., Casares, J. A., Jimenez, M. V., Meli, A., Moneti, S., Vizza, F., Herrera, V. and

Sánchez-Delgado, R., *Organometallics* 1995, **14,** 4850.

32. Chen, J., Daniels, L. M. and Angelici, R. J., *Polyhedron* 1990, **9,** 1883.
33. Bianchini, C., Meli, A., Peruzzini, M., Vizza, F., Frediani, P., Herrera, V. and Sánchez-Delgado, R. A., *J. Am. Chem. Soc.* 1993, **115,** 2731.
34. Curtis, M. D., *Appl. Organomet. Chem.* 1992, **6,** 429.
35. Durker S. H. and Curtis, M. D., *J. Am. Chem. Soc.* 1995, **117,** 6366.
36. Curtis, M. D., Riaz, U., Curnow, O. J., Kampf, J. W., Rheingold, A. L. and Haggerty, B. S., *Organometallics* 1995, **14,** 5337.
37. Bergert, L. and Harris, S., manuscript in preparation.
38. Harris, S., *Inorg. Chem.* 1987, **26,** 4278.
39. Harris, S., *Polyhedron* 1989, **8,** 2843.
40. Curnow, O. J., Kampf, J. W. and Curtis, M. D., *Organometallics* 1992, **11,** 1984.
41. Curnow, O. J., Kampf, J. W., Curtis, M. D., Shen, J. and Basolo, F., *J. Am. Chem. Soc.* 1994, **116,** 224.
42. Murata, T., Mizobe, Y., Gao, H., Ishii, Y., Wakabayashi, T., Makano, F., Tanase, T., Yano, S., Hidai, M., Echizen, I., Nanikawa, H. and Motomura, S., *J. Am. Chem. Soc.* 1994, **116,** 3389.
43. Saysell, D. M., Borman, C. D., Kwak, C.-H. and Sykes, A. G., *Inorg. Chem.* 1996, **35,** 173.
44. Schmidt, I., Hyldtoft, J., Hjortkjaer, J. and Jacobsen, C. J. H., *Acta Chim. Scandinavica*, 1996, **50,** 871.